Supporting information

Improving Cycling Stability of the Lithium Anode by a Spin-Coated High-Purity Li_3PS_4 Artificial SEI Layer

Hongjiao Wang[a,b], Lilin Wu[c], Bai Xue[a], Fang Wang[c], Zhongkuan Luo[c], Xianghua Zhang[b], Laurent Calvez[b], Ping Fan[a]*, Bo Fan[a,]*

a. Shenzhen Key Laboratory of Advanced Thin Films and Applications, College of Physics and Optoelectronic Engineering, Shenzhen University, Shenzhen 518060, Guangdong, China.

b. Laboratory of Glasses and Ceramics, Institute of Chemical Science, University of Rennes 1, Rennes 35042.

c. College of Chemistry and Environmental Engineering, Shenzhen University, Shenzhen 518060, Guangdong, China.

*Corresponding author E-mail addresses: fanping@szu.edu.cn (Ping Fan), fanb07@hotmail.com (Bo Fan).

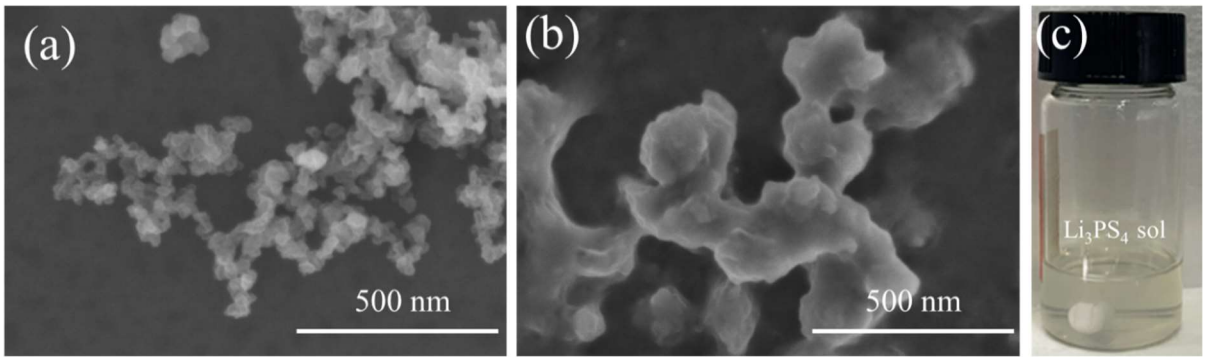

Figure S1. SEM images of (a) the Li_2S nanoparticles and (b) Li_3PS_4 nanoparticles. (c) photograph of the as-prepared Li_3PS_4 sol.

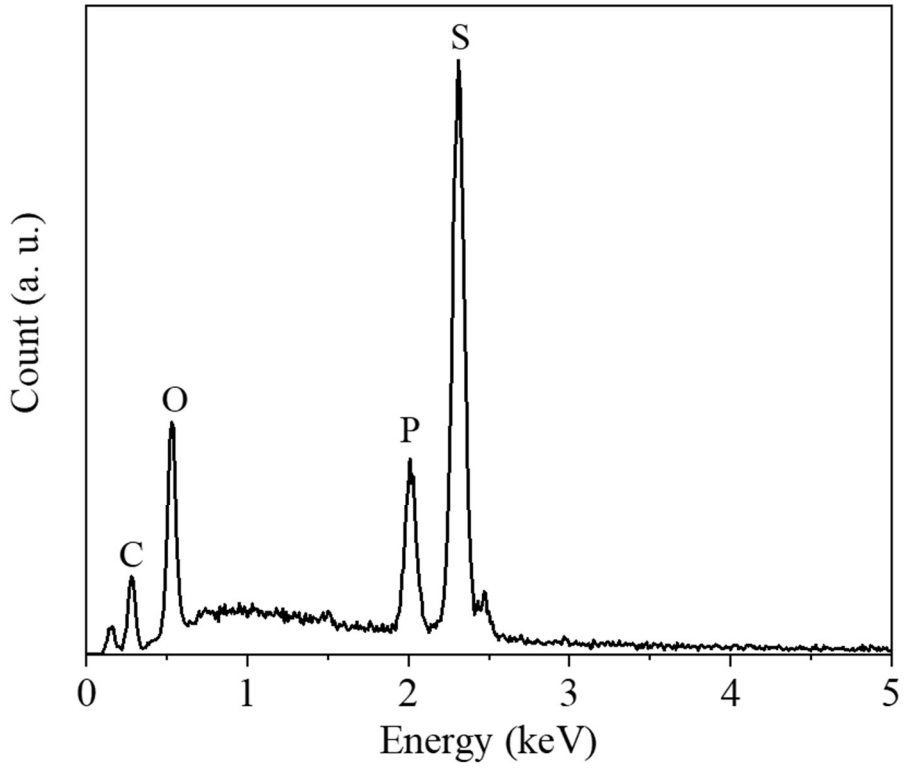

Figure S2. EDS spectrum of the Li_3PS_4-protected lithium electrode.

Table S1. Elemental analysis of the Li_3PS_4-protected lithium electrode.

elements	atomic %
C	34.18
O	34.15
P	7.26
S	24.41
Total	100.00

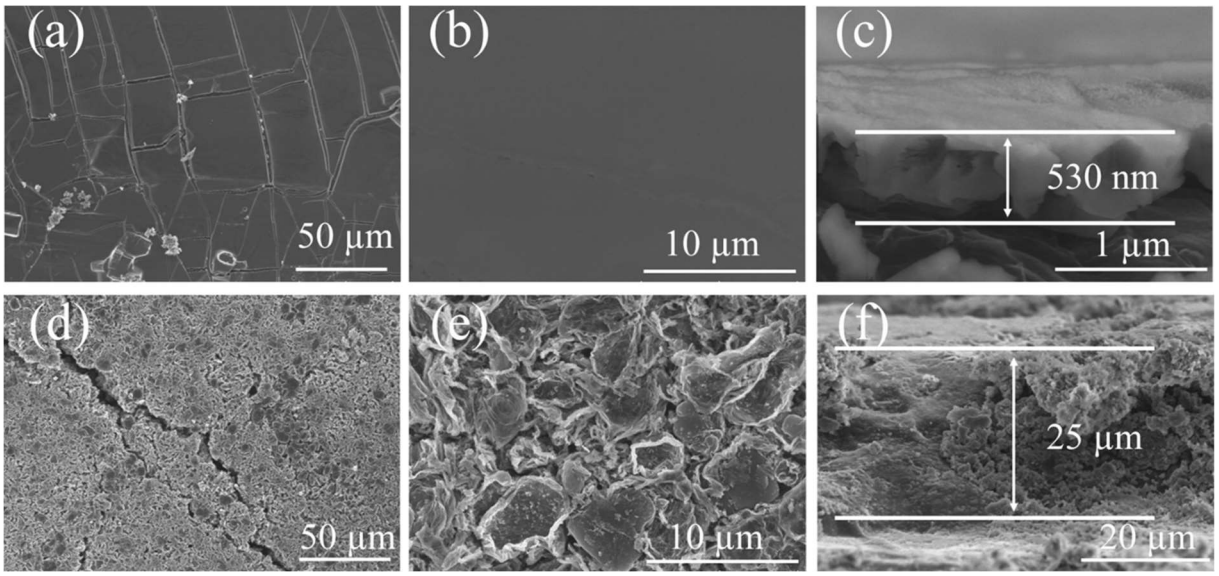

Figure S3. Characterization of the Li/LPS-0.1M electrodes before and after 500 h cycling at a current density of 1 mA cm^{-2} and with a capacity density of 1 mA h cm^{-2}. (a, b) Top-view and (c) cross-sectional SEM images of the pristine Li/LPS-0.1M electrode. (d, e) Top-view and (f) cross-sectional SEM images of the Li/LPS-0.1M electrode after cycling.

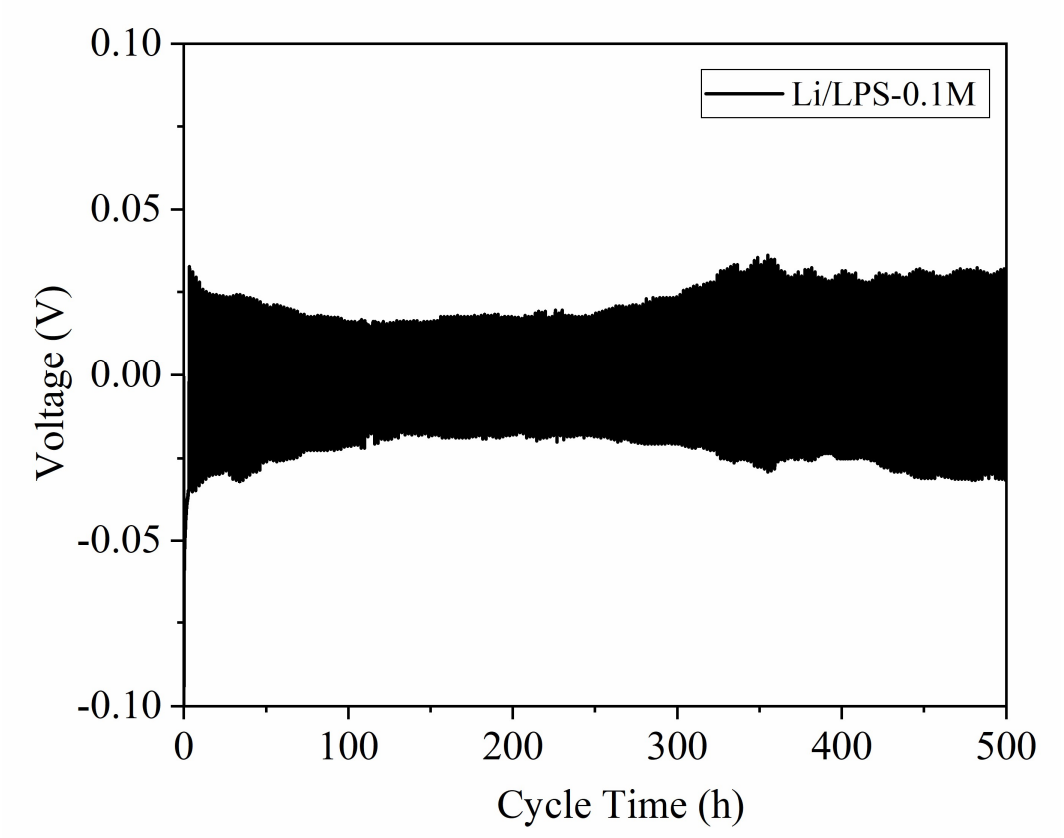

Figure S4. Long-term cycling performance of the Li/LPS-0.1M symmetrical cell at a current density of 1 mA cm^{-2} with a capacity density of 1 mA h cm^{-2}.

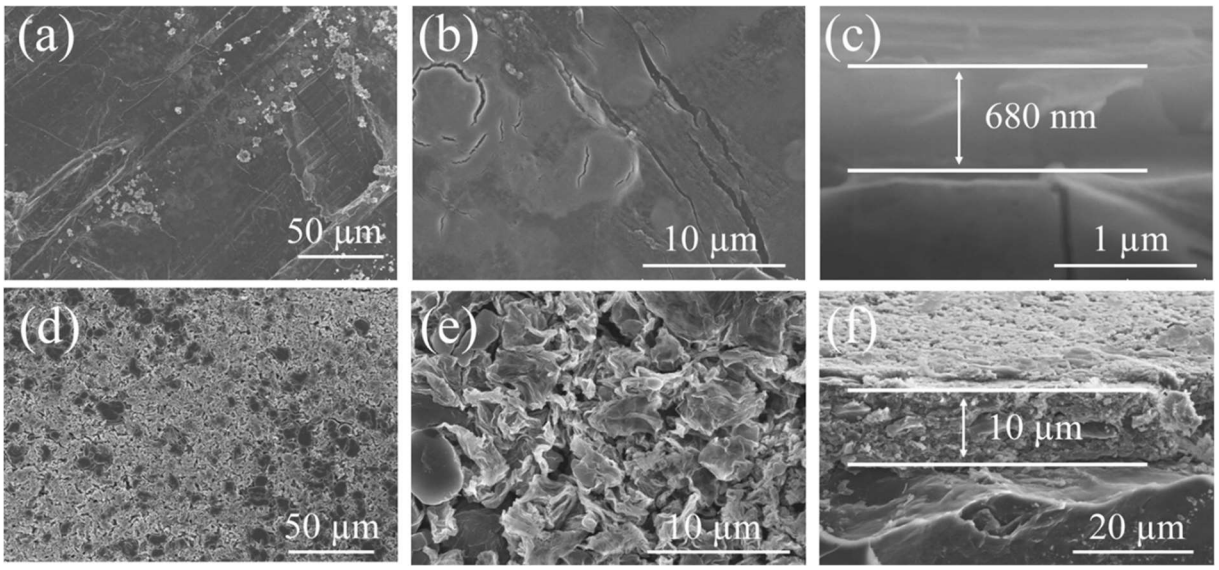

Figure S5. Characterization of the Li/LPS-0.08M electrodes before and after 500 h cycling at a current density of 1 mA cm^{-2} and with a capacity density of 1 mA h cm^{-2}. (a, b) Top-view and (c) cross-sectional SEM images of the pristine Li/LPS-0.08M electrode. (d, e) Top-view and (f) cross-sectional SEM images of the Li/LPS-0.08M electrode after cycling.

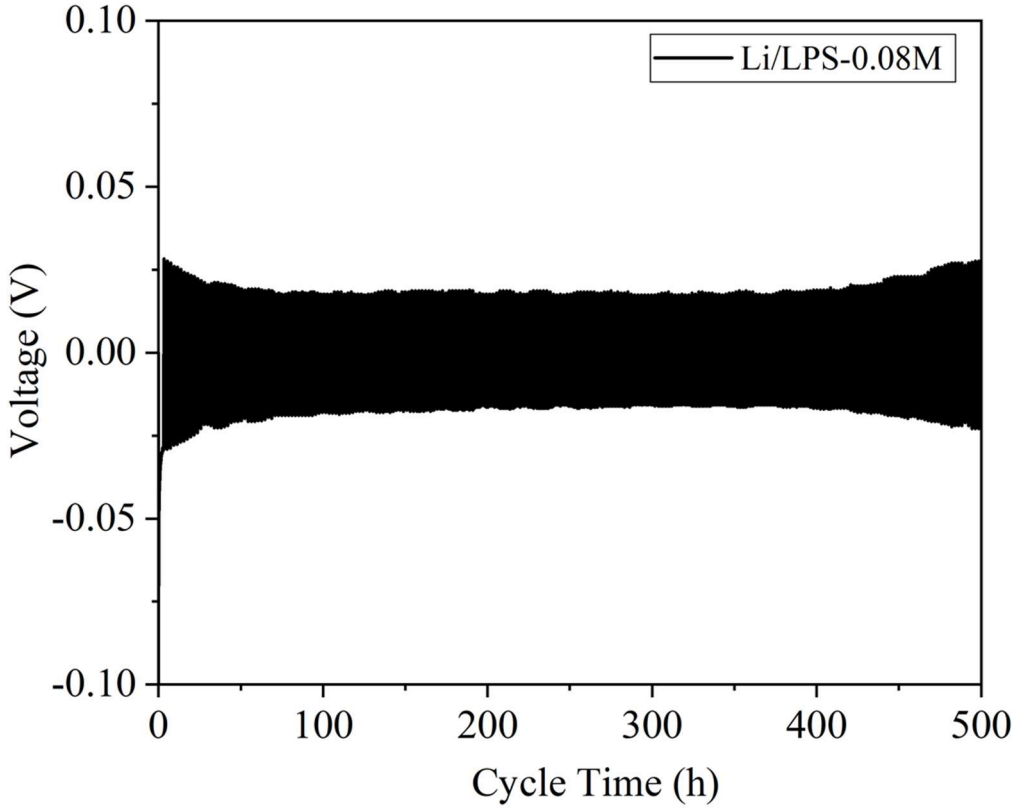

Figure S6. Long-term cycling performance of the Li/LPS-0.08M symmetrical cells at the current density of 1 mA cm^{-2} with a capacity density of 1 mA h cm^{-2}.

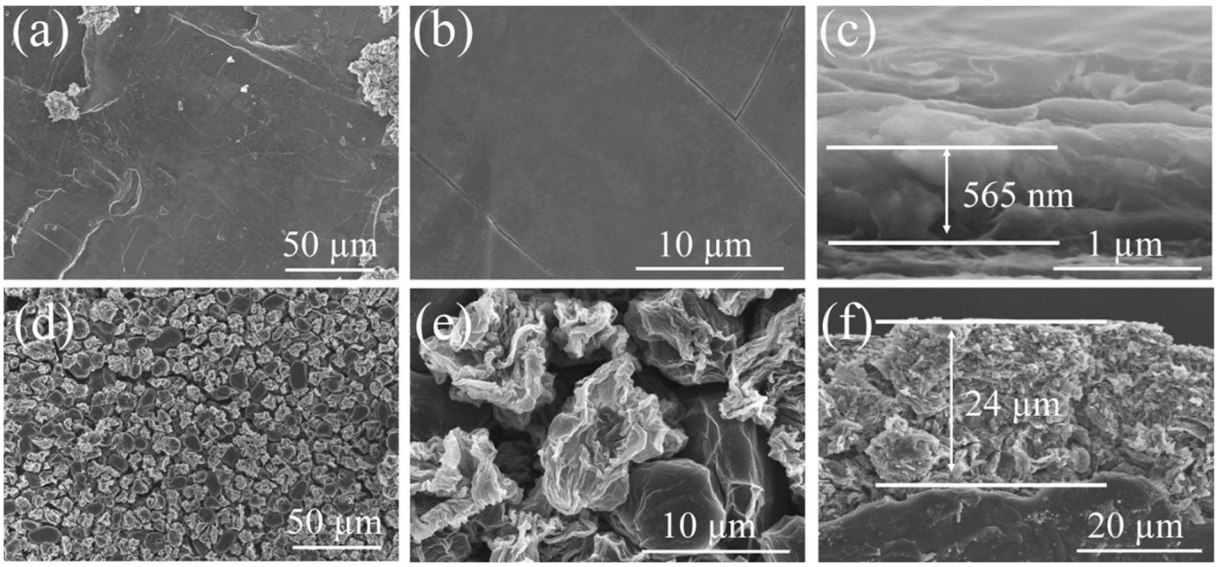

Figure S7. Characterization of the Li/LPS-0.04M electrodes before and after 500 h cycling at a current density of 1 mA cm^{-2} and with a capacity density of 1 mA h cm^{-2}. (a, b) Top-view and (c) cross-sectional SEM images of the pristine Li/LPS-0.04M electrode. (d, e) Top-view and (f) cross-sectional SEM images of the Li/LPS-0.04M electrode after cycling.

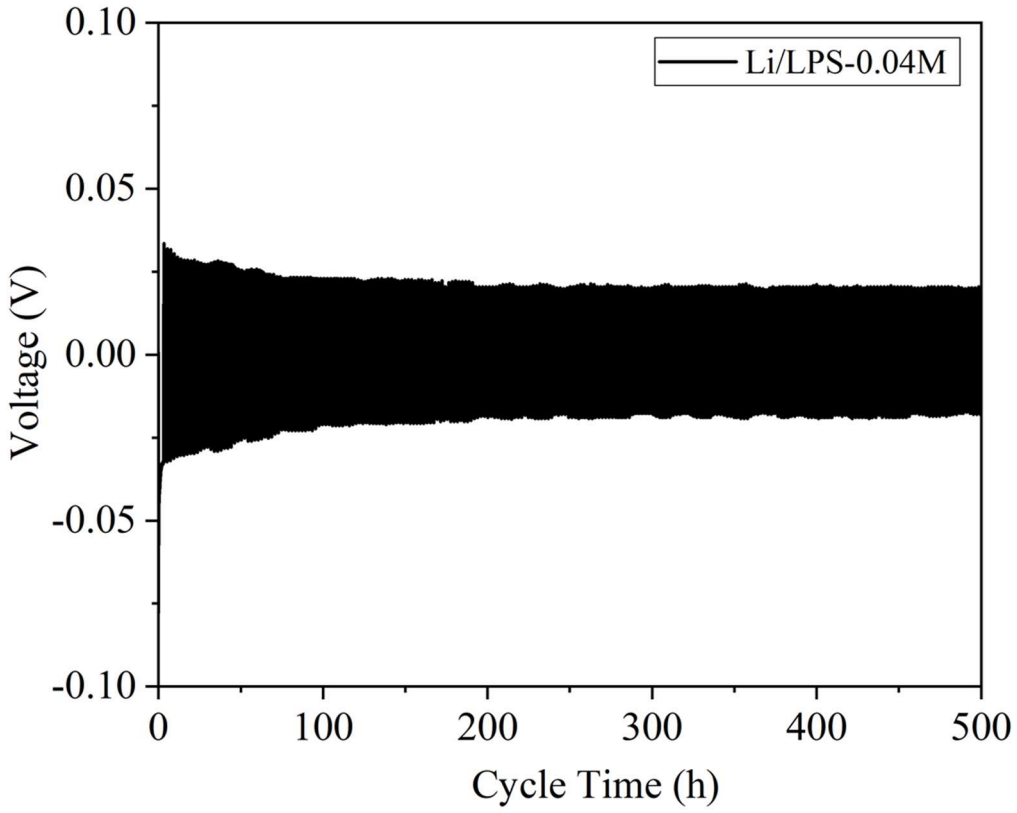

Figure S8. Long-term cycling performance of the Li/LPS-0.04M symmetrical cells at the current density of 1 mA cm^{-2} with a capacity density of 1 mA h cm^{-2}.

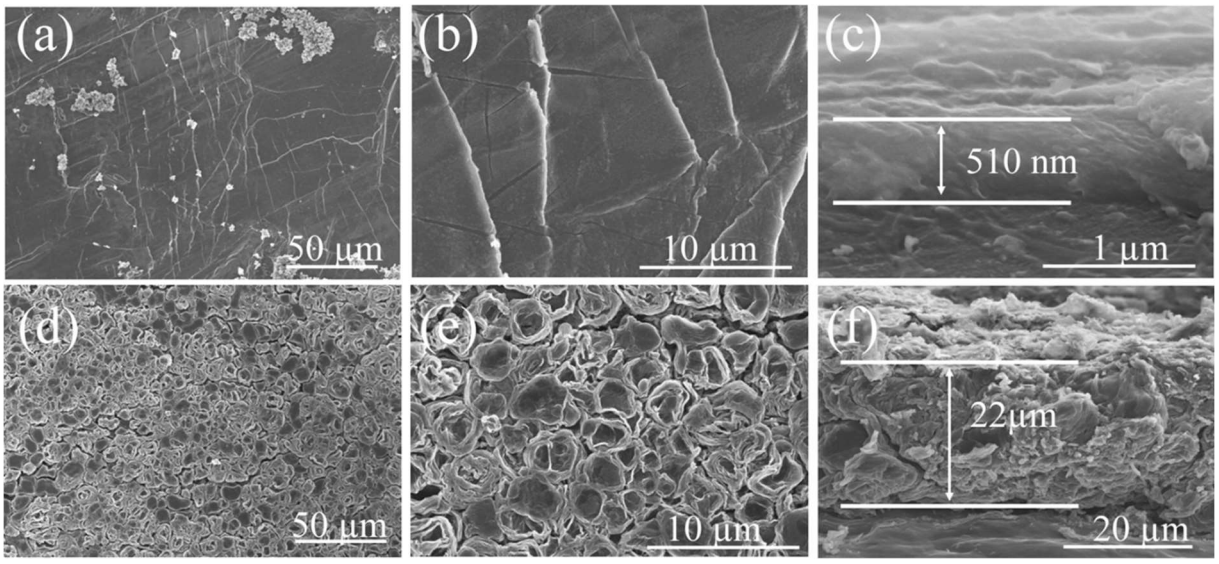

Figure S9. Characterization of the Li/LPS-0.02M electrodes before and after 500 h cycling at a current density of 1 mA cm^{-2} and with a capacity density of 1 mA h cm^{-2}. (a, b) Top-view and (c) cross-sectional SEM images of the pristine Li/LPS-0.02M. (d, e) Top-view and (f) cross-sectional SEM images of the Li/LPS-0.02M electrode after cycling.

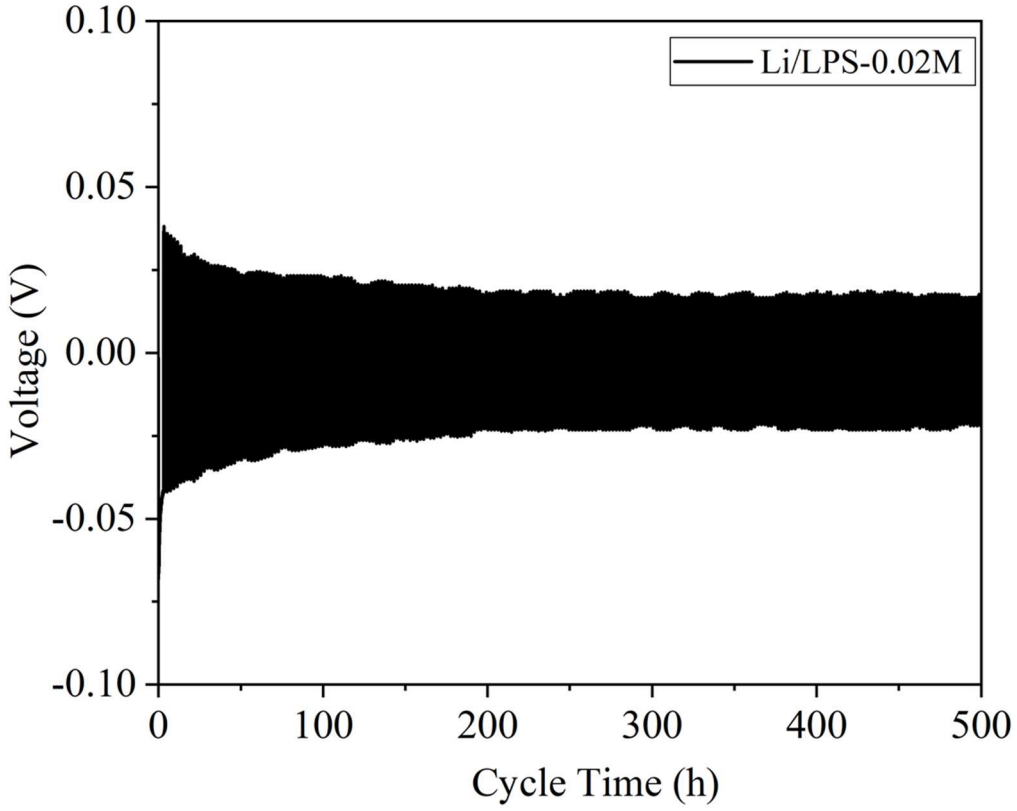

Figure S10. Long-term cycling performance of the Li/LPS-0.02M symmetrical cells at the current density of 1 mA cm^{-2} with a capacity density of 1 mA h cm^{-2}.

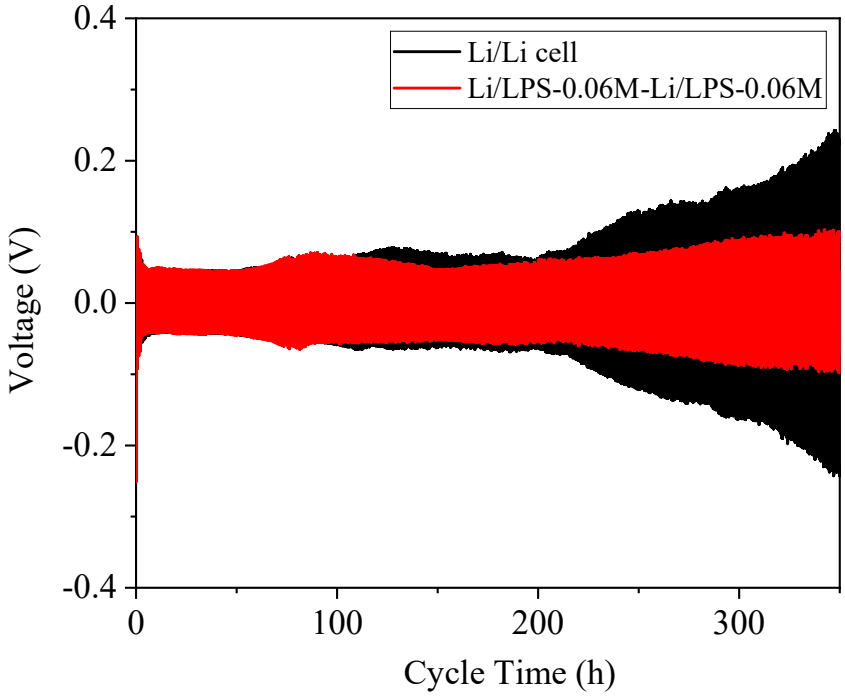

Figure S11. Long-term cycling performance of the bare Li and Li/LPS-0.06M symmetrical cells at a current density of 3 mA cm^{-2} with a capacity density of 1 mA h cm^{-2}.

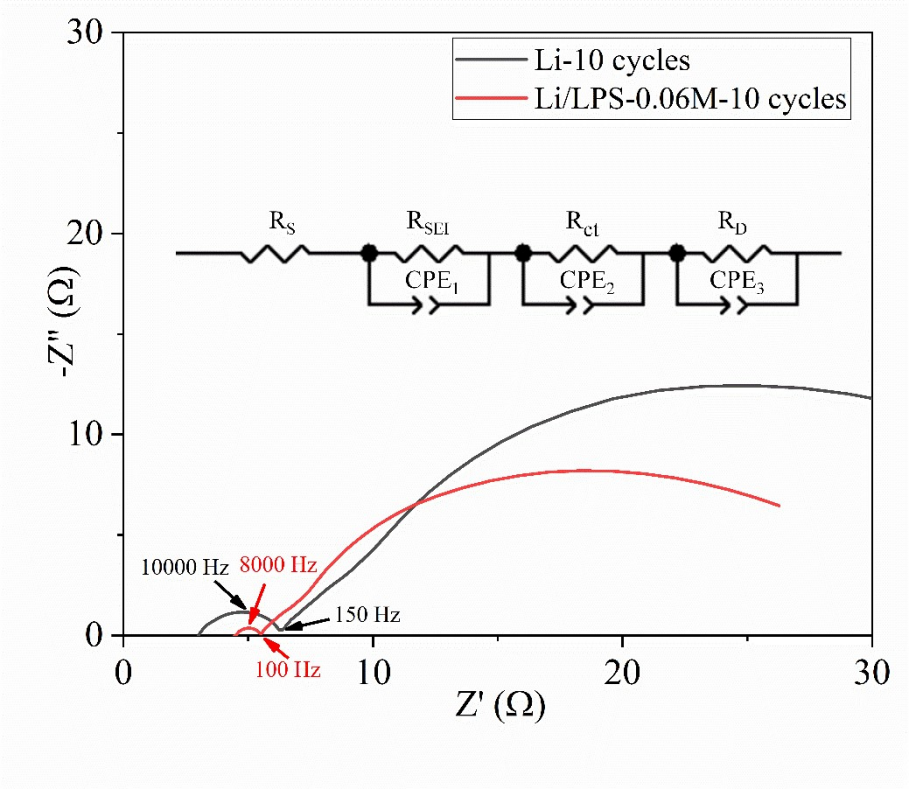

Figure S12. Electrochemical impedance spectroscopy of (a) the Li symmetrical cell and (b) the Li/LPS-0.06M symmetrical cell after 10 cycles. The inset shows the corresponding equivalent circuit model, where R_s, R_{SEI} and R_{ct}, represent the resistance

of the solution, SEI film, and charge transfer process. The parallel R_D is used to fit the low-frequency tail caused by the lithium-ion diffusion. This treatment is for simplifying the fitting.

Table S2. Fitted R_s, R_{SEI}, and R_{ct} of the symmetrical cells with the bare Li and Li/LPS-0.06M electrodes after 10 cycles.

Material	R_s (Ω)	R_{SEI} (Ω)	R_{ct} (Ω)
Li	3.3	2.9	2.3
Li/LPS-0.06M	4.6	0.8	0.9

Table S3. Comparison of the Li symmetrical batteries with Li_3PS_4-based artificial SEI and other SEI strategies.

SEI strategy	current density (mA cm^{-2})	capacity (mA h cm^{-2})	cycle Life (h)	overpotential (mV)	ref.
Li_3PS_4	1.0	1.0	800	25	this
	3.0	1.0	350	100	work
P_2S_5/S	1.0	1.0	100	25	1
P_4S_{10}	1.0	1.0	270	25	2
	2.0	2.0	100	50	
P_4S_{16}	0.5	1.0	2000	25	3
	1.0	1.0	not given	100	
Sn-coating	1.0	1.0	900	25	4
	3.0	1.0	100	80	
3D electrode	1.0	1.0	350	50	5

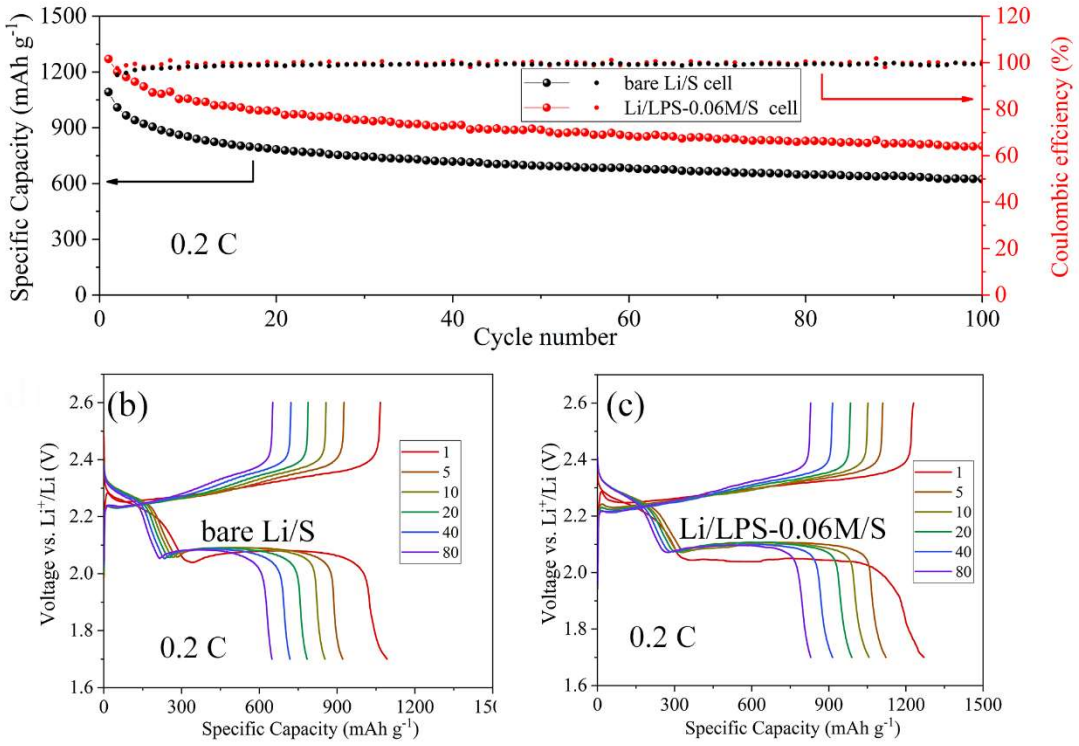

Figure S13. Electrochemical performance of the Li-S batteries with the Li/LPS-0.06M and bare Li anodes. (a) Discharge capacity and coulombic efficiency at 0.2 C; (b, c) Galvanostatic charge/discharge curves of the Li/LPS-0.06M/S and Li/S batteries at 0.2 C. (1 C = 1675 mA g^{-1})

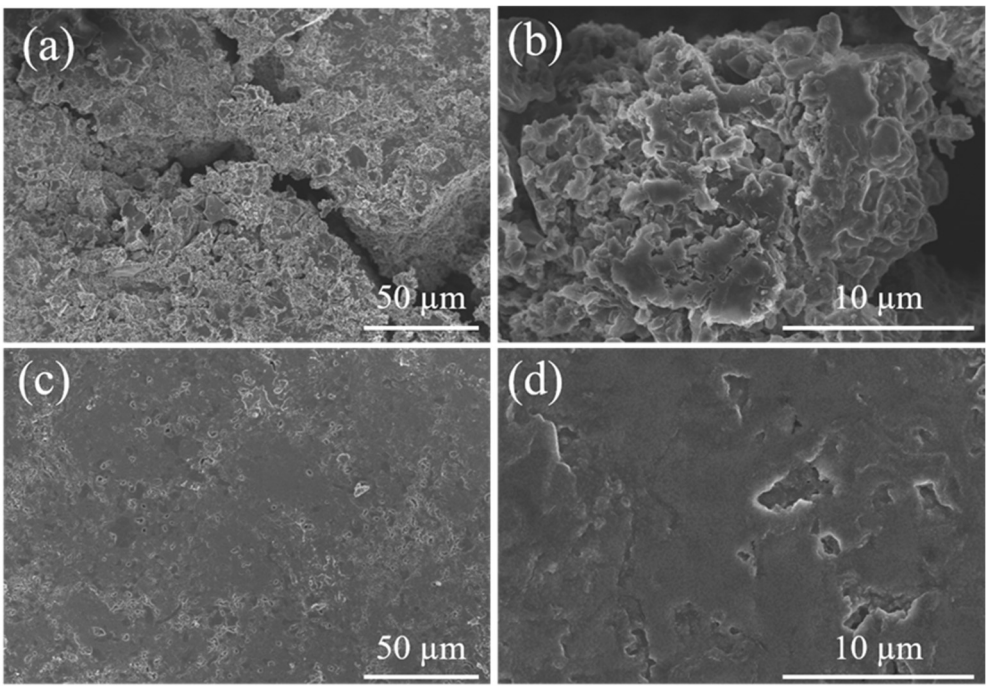

Figure S14. Characterization of the bare Li and Li/LPS-0.06M electrodes after 145 cycles in the Li-LFP battery at 1C. (a, b) SEM images of the bare Li electrode after cycling. (c, d) SEM images of the Li/LPS-0.06M electrode after cycling.

Reference

(1) Lu, Y.; Gu, S.; Hong, X.; Rui, K.; Huang, X.; Jin, J.; Chen, C.; Yang, J.; Wen, Z., Pre-modified Li_3PS_4 Based Interphase for Lithium Anode Towards High-performance Li-S Battery. *Energy Storage Mater.* **2018,** *11*, 16-23.
(2) Li, M.; Liu, X.; Li, Q.; Jin, Z.; Wang, W.; Wang, A.; Huang, Y.; Yang, Y., P_4S_{10} Modified Lithium Anode for Enhanced Performance of Lithium–sulfur Batteries. *J. Energy. Chem.* **2020,** *41*, 27-33.
(3) Liang, J.; Li, X.; Zhao, Y.; Goncharova, L. V.; Wang, G.; Adair, K. R.; Wang, C.; Li, R.; Zhu, Y.; Qian, Y.; Zhang, L.; Yang, R.; Lu, S.; Sun, X., In Situ Li_3PS_4 Solid-State Electrolyte Protection Layers for Superior Long-Life and High-Rate Lithium-Metal Anodes. *Adv. Mater.* **2018,** *30*, article no. e1804684.
(4) Xia, S.; Zhang, X.; Liang, C.; Yu, Y.; Liu, W., Stabilized Lithium Metal Anode by an Efficient Coating for High-performance Li–S Batteries. *Energy Storage Mater.* **2020,** *24*, 329-335.
(5) Yang, T.; Sun, Y.; Qian, T.; Liu, J.; Liu, X.; Rosei, F.; Yan, C., Lithium Dendrite Inhibition via 3D Porous Lithium Metal Anode Accompanied by Inherent SEI Layer. *Energy Storage Mater.* **2020,** *26*, 385-390.